http://dergipark.org.tr/trkjnat
Trakya University Journal of Natural Sciences, 25(1): 97-110, 2024
ISSN 2528-9691
DOI: 10.23902/trkjnat.1446327

Research Article

Amanita vidua: A new record for Turkish *Amanita* Section *Phalloideae* based on morphological and molecular data

Ilgaz AKATA[1*], Eda KUMRU[2], Ergin ŞAHİN[3-4], İsmail ACAR[5-6], Ertuğrul KAYA[7]

[1] Ankara University, Faculty of Science, Department of Biology, Ankara, TÜRKİYE
[2] Ankara University, Graduate School of Natural and Applied Sciences, Ankara, TÜRKİYE
[3] Dokuz Eylül University, Faculty of Science, Department of Biology, İzmir, TÜRKİYE
[4] Dokuz Eylül University, Fauna and Flora Research and Application Center, İzmir, TÜRKİYE
[5] Van Yüzüncü Yıl University, Başkale Vocational High School, Department of Organic Agriculture, Van, TÜRKİYE
[6] Çanakkale Onsekiz Mart University Çanakkale Vocational School of Health Services, Department of Medical Services and Techniques, Çanakkale, TÜRKİYE
[7] Niğde Ömer Halisdemir University, Faculty of Medicine, Department of Internal Medical Sciences, Niğde, TÜRKİYE

Cite this article as:

Akata I., Kumru E., Şahin E., Acar İ. & Kaya E. 2024. *Amanita vidua*: A new record for Turkish *Amanita* Section *Phalloideae* based on morphological and molecular data. *Trakya Univ J Nat Sci*, 25(1): 97-110, DOI: 10.23902/trkjnat.1446327

Received: 02 March 2024, Accepted: 30 March 2024, Online First: 09 April 2024, Published: 15 April 2024

Edited by:
Boris Assyov

***Corresponding Author:**
Ilgaz Akata
akata@science.ankara.edu.tr

ORCID iDs of the authors:
IA. 0000-0002-1731-1302
EK. 0009-0000-7417-6197
EŞ. 0000-0003-1711-738X
İA. 0000-0002-6049-4896
EK. 0000-0003-0081-682X

Key words:
Amanitaceae
Mycobiota
Asia Minor
Türkiye

Abstract: In the present study, fungal specimens collected from Yeşildere village in Uşak province, Türkiye were evaluated. The specimens underwent detailed examination through both morphological and DNA (nrITS rDNA region and *TEF1a* gene) sequence-based phylogenetic analysis. Based on the evaluation of micro- and macromorphological characteristics, and phylogenetic analyses, the specimen was identified as *A. vidua* Gasch, G. Moreno & P.-A. Moreau. This identification marks *A. vidua* as a new record for the Turkish *Amanita* section *Phalloideae*. The study described this newly recorded species, including specific details such as its location, habitat observations, geographical coordinates, collection date, and photographs showcasing its macro and micromorphological features. Additionally, it also includes illustrations of some microscopic structures of the species. The study is further enriched with SEM images, offering a detailed view of the species characteristics, and the findings are briefly discussed.

Özet: Bu çalışmada Türkiye'nin Uşak iline bağlı Yeşildere Köyü'nden toplanan mantar örnekleri değerlendirilmiştir. Bu örnekler hem morfolojik hem de DNA (nrITS rDNA bölgesi ve *TEF1a* geni) dizisine dayalı filogenetik analiz yoluyla ayrıntılı incelemeye tabi tutulmuştur. Mikro ve makromorfolojik özelliklerin değerlendirilmesi ve filogenetik analizlere dayanarak örnek *A. vidua* Gasch, G. Moreno & P.-A. Moreau olarak tanımlanmıştır. Bu tanımlama, *A. vidua'* yı Türkiye'deki *Amanita* cinsinin *Phalloideae* seksyonu için yeni bir kayıt olarak belirlenmiştir. Çalışma, yeni kaydedilen bu türün konumu, habitat gözlemleri, coğrafi koordinatları, toplanma tarihi ve makro ve mikromorfolojik özelliklerini gösteren fotoğraflar gibi belirli ayrıntıları içeren bir tanımını sunmaktadır. Ayrıca türün bazı mikroskobik yapılarına ait çizimler de yer almaktadır. Çalışma, türün karmaşık özelliklerinin ayrıntılı bir görünümünü sunan taramalı elektron mikroskobundan (SEM) elde edilen görüntülerle daha da zenginleştirilmiştir ve bu bulgular kısaca tartışılmıştır.

Introduction

The genus *Amanita* Pers., belonging to the family *Amanitaceae* E.-J. Gilbert, includes about 700 accepted species out of approximately 1000 named taxa in scientific literature (Codjia *et al.* 2022). The genus is remarkable for its array of species, ranging from highly edible to extremely toxic ones. A majority of *Amanita* species engage in ectomycorrhizal relationships with vascular plants, contributing vitally to ecosystem health (Corrales *et al.* 2018, Codjia *et al.* 2022). In terms of classification, recent advancements that incorporate both morphological features and genetic analysis have led to the division of *Amanita* into three subgenera, further subdivided into eleven sections (Cui *et al.* 2018). Among these, *Amanita* sect. *Phalloideae* (Fr.) Quél. is widely known and comprises about 70 identified species (Thongbai *et al.* 2017, Fraiture *et al.* 2019, Codjia *et al.* 2020), of which more than 50 are extremely toxic species, containing lethal compounds such as amatoxins, phallotoxins, and virotoxins (Thongbai *et al.* 2017, Codjia *et al.* 2022).

Taxonomic studies on the mycobiota of Türkiye have reported 39 *Amanita* species so far (Sesli 2022, Sesli *et al.* 2020). Within the *Amanita* sect. *Phalloideae*, three distinct species, *A. phalloides* (Vaill. ex Fr.) Link, *A. verna* Bull. ex Lam., and *A. virosa* Bertill, are present in the country, *Amanita vidua* Gasch, G. Moreno & P.-A. Moreau, another species in the *Amanita* sect. *Phalloideae*, has not been documented in the Turkish mycobiota so far (Akata *et al.* 2015, Sesli *et al.* 2020).

The present study aimed to contribute to Turkish *Amanita* diversity.

Materials and Methods

Fungal samples collected from the designated study area of Yeşildere village (Uşak-Türkiye) dominated by *Quercus ithaburensis* Decne subsp. *macrolepis* (Kotschy) Hedge & Yalt. (Figs 1, 2) on June 2, 2023, was included in the study. Conventional and advanced molecular techniques were used in an integrative manner for the identification and classification of the collected samples. Macroscopic and microscopic evaluation of the samples was complemented by the sequence comparison and phylogenetic analysis of nrITS rDNA and translation elongation factor 1 alpha (*TEF1a*) gene sequences.

Morphological Characterization

After their collection, fungal samples underwent a thorough examination of their macroscopic characteristics and environmental conditions directly at the site. Within the laboratory, the samples were further scrutinized under a light microscope (Euromex Oxion) to investigate their fine details. Each microscopic feature was measured approximately 30 times to ensure the accuracy of the results. Melzer's reagent, 5% potassium hydroxide (KOH), and Congo red were utilized for the analytical process.

For scanning electron microscope (SEM) analysis, small fragments of the samples were affixed to stubs using double-sided adhesive tape and were gold-coated. The examination was carried out using an EVO 40XVP SEM, produced by LEO Ltd. in Cambridge, UK. This device was operated at an accelerating voltage of 20 kV.

The identification of the samples' morphology was performed by the methodologies delineated by Alvarado *et al.* (2022). This particular study was pivotal in offering detailed and systematic protocols essential for the precise identification of the samples. Following their identifications, the samples were preserved at the Fungarium in Ankara University, and deposited in the Science Faculty, Department of Biology.

Fig. 1. Collection area. **a-c**. General appearance, **d.** leaves of *Quercus ithaburensis* subsp. *macrolepis*.

Determination of the ITS rDNA and TEF1a Sequences

The genomic DNA was extracted from the sample ANK Akata & Kaya 007 using the CTAB method, following the protocol of Rogers & Bendich (1994). The quality and quantity of the isolated genomic DNA were assessed using a Nanodrop Lite device manufactured by Thermo Fisher Scientific. The extracted DNA was used as a template in a polymerase chain reaction (PCR) to amplify the Internal Transcribed Spacer (ITS) rDNA (White *et al.* 1990) and *TEF1a* gene regions. In PCR amplification of ITS, primer pairs ITS1: 5'-TCCGTAGGTGAACCTGCGG-3' and ITS4: 5'-TCCTCCGCTTATTGATATGC-3 were used following a previously described protocol (Martin & Rygiewicz 2005). In PCR amplification of the *TEF1a* gene, the EF1-983F: 5'-GCYCCYGGHCAYCGTGAYTTYAT-3' and EF1-1567R: 5'-ACHGTRCCRATACCACCRATCTT-3' primer couple was used as described elsewhere (Rehner & Buckley 2005). The presence of the amplification product (amplicon) was confirmed through agarose gel electrophoresis. The amplicon was then purified using the GeneAll Expin Gel, PCR, and CleanUp SV Kit and then subjected to Sanger dideoxy sequencing. For sequencing PCR, the same ITS1/ITS4 and EF1-983F/EF1-1567R primer pairs were used, utilizing the BigDye™ Direct Cycle Sequencing Kit by Thermo Fisher Scientific. Fragment analysis was performed using the ABI Prism 3130 Genetic Analyzer. The procedures of agarose gel electrophoresis and Sanger sequencing were carried out following the methods described previously (Chen *et al.* 2014).

Molecular Phylogeny

In order to obtain data for presentation of molecular phylogeny, the Sanger sequencing reads obtained from the ITS1/ITS4 and EF1-983F/EF1-1567R primer pairs were assembled using DNAMAN ver. 10, a sequence assembly software by Lynnon Corporation. BLASTn analyses were performed on the assembled sequences to determine their identity rates. Based on the results of these BLAST analyses, the ingroup and outgroup members for phylogenetic analyses were retrieved from the NCBI GenBank database. The assembled sequences were then aligned with the nucleotide sequences of the retrieved ingroup and outgroup members using the ClustalW algorithm, which is part of the MEGAX software (Kumar *et al.* 2018). To unveil the evolutionary history of the Turkish collection inferred from ITS rDNA and *TEF1a* gene sequences, T92 with uniform rates and K2+I nucleotide substitution models were used respectively to construct phylogenetic trees with the Maximum Likelihood method (Kimura 1980, Tamura 1992). To assess accuracy, the bootstrap method was applied with 1000 bootstrap replicates, as previously described (Felsenstein 1985).

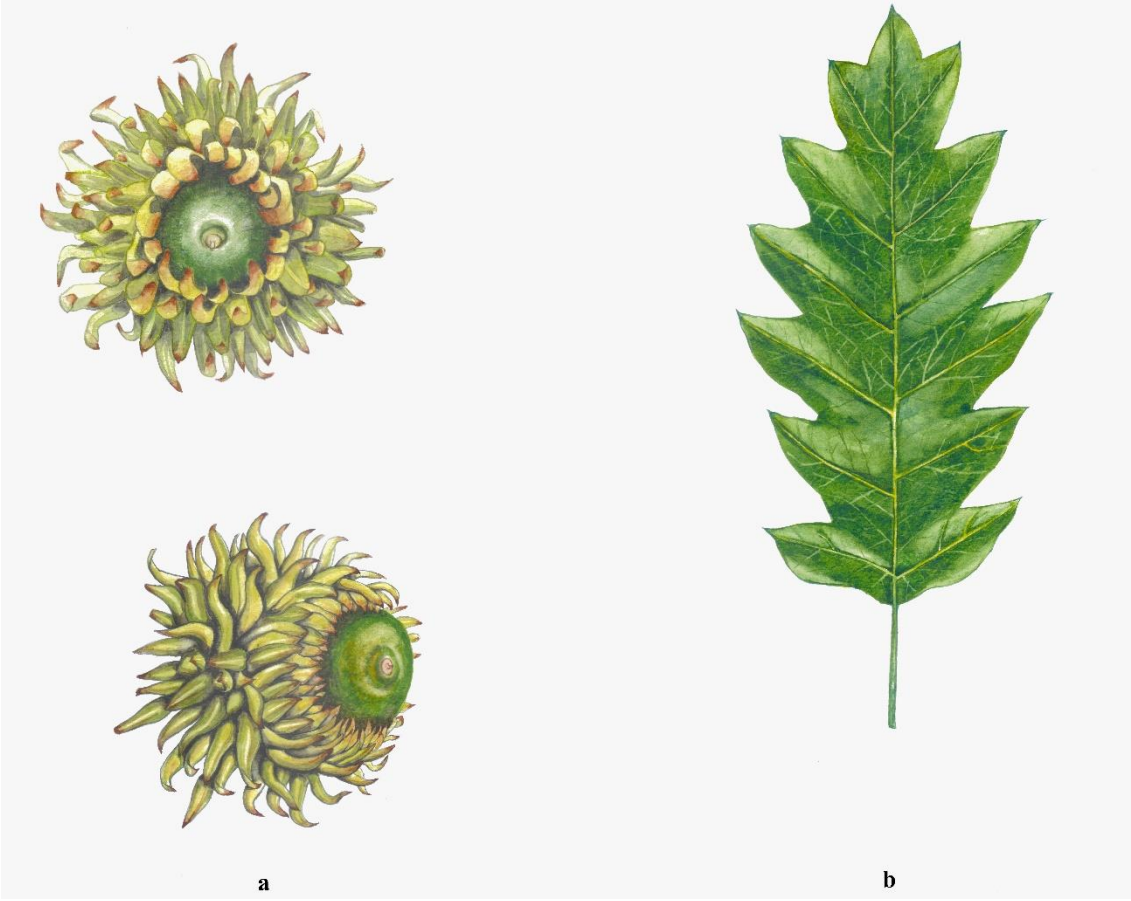

Fig. 2. *Quercus ithaburensis* subsp. *macrolepis*. **a.** Acorns, **b.** leaf (Illustrated by Meltem Kurt).

Results

The collected fungal samples were identified as *Amanita vidua*. A description of the identified species, based on both the macroscopic and microscopic morphological features of the samples, is presented along with information on the date of collection, specific location, habitat observation, geographical coordinates, and collection identifiers. SEM images of the spores, which offer a more detailed insight into the complex characteristics of the species were also provided.

Amanita vidua Gasch, G. Moreno & P.-A. Moreau (2022) (Figs 1-9).

A detailed description of the type specimens in the original collections is provided by Alvarado *et al.* (2022).

Macroscopic and microscopic features

Pileus 60-80 mm across, somewhat spherical to hemispherical but later expanding to convex or flat, with a small umbo. **Surface** whitish to cream in color, occasionally with yellowish or ochre-pinkish shades at the center, smooth and shiny; remnants of the universal veil on pileus absent. **Margin** lacks any striation, initially inrolled but later flattened and eventually turned upwards, remaining smooth and the same color as the rest of the pileus. **Lamellae** close to crowded, free, white to whitish cream, smooth, sometimes with fine hairs or serrations, with concolorous and rounded lamellulae. **Stipe** 90-130 × 14-19 mm, white to whitish, cylindrical, slightly widening towards the base, smooth above the annulus, smooth to pruinose-floccose below. **Annulus** well-developed, white and membranous, sometimes with the appearance of having a dual ring because of the presence of a slanting band located a few millimeters below **Volva** sack-like, membranous, white. **Context** thin, whitish to cream. **Odor** and **taste** fungoid. **Spore** print white. **Basidiospores** (9.7-) 9.9-11.8 (-12.3) × (7.8-) 8-9 (-9.4) µm, Q = 1.16-1.40 (-1.47), Qav = 1.32, subglobose to broadly ellipsoid, smooth, hyaline, amyloid. **Basidia** 42-64 × 13-18 µm, cylindrical to clavate, four spored, without clamp connections. **Subhymenium** lobate, rounded, or broadly elliptical, sometimes angular or cordiform structures measuring 17-32 × 13-24 µm. **Hymenophoral trama** bilateral, divergent, with a central strand densely packed and composed of slender, parallel, filamentous hyphae measuring 3-5 µm, intermingled with wide, expanded hyphae measuring 8-12 µm**. Lamellar edge** fertile, containing clavate to capitate terminal cells, measuring 29-41 × 15-18 µm. **Partial veil (annulus)** composed of complex, hyaline, cylindrical hyphae 4-8 µm, characterized by a smooth texture, absence of clamp connections, and wall thicknesses reaching up to 2 µm, the upper surface made up of filamentous structures, randomly dotted with clavate or spherical-stalked components measuring 22-45 × 8-16 µm. **Universal veil (volva)** composed of two layers; the inner layer characterized by delicate, filamentous structures consisting of complex, cylindrical hyphae in 3-9 µm length, occasionally branched and without clamp connections, mixed with sparsely less densely packed, somewhat swollen elements up to 20 µm; the outer layer formed by thin, cylindrical hyphae up to 9 µm broad, in KOH exhibiting a yellowish hue, with areas adorned with yellowish encrustations. **Pileipellis** consisting of two layers; suprapellis ixocutis, composed of gelatinized filamentous hyphae measuring 2-5 µm, without clamp connections and certain hyphae containing yellow granular material observed in KOH, subpellis not gelatinized and structurally similar to the suprapellis, primarily consisting of parallel, slender hyphae measuring 2-5 µm, some wider hyphae measuring up to 10 µm broad; walls with a yellowish tint. **Terminal cells of subpellis** of extended shape, varying from cylindrical to spathulate or obovate, with apex either rounded or narrowly pointed, measuring 75-160 × 12-32 µm.

Fig. 3. Basidiomata of *Amanita vidua* (Illustrated by Meltem Kurt).

Fig. 4. *Amanita vidua*. **a-f.** Basidiomata.

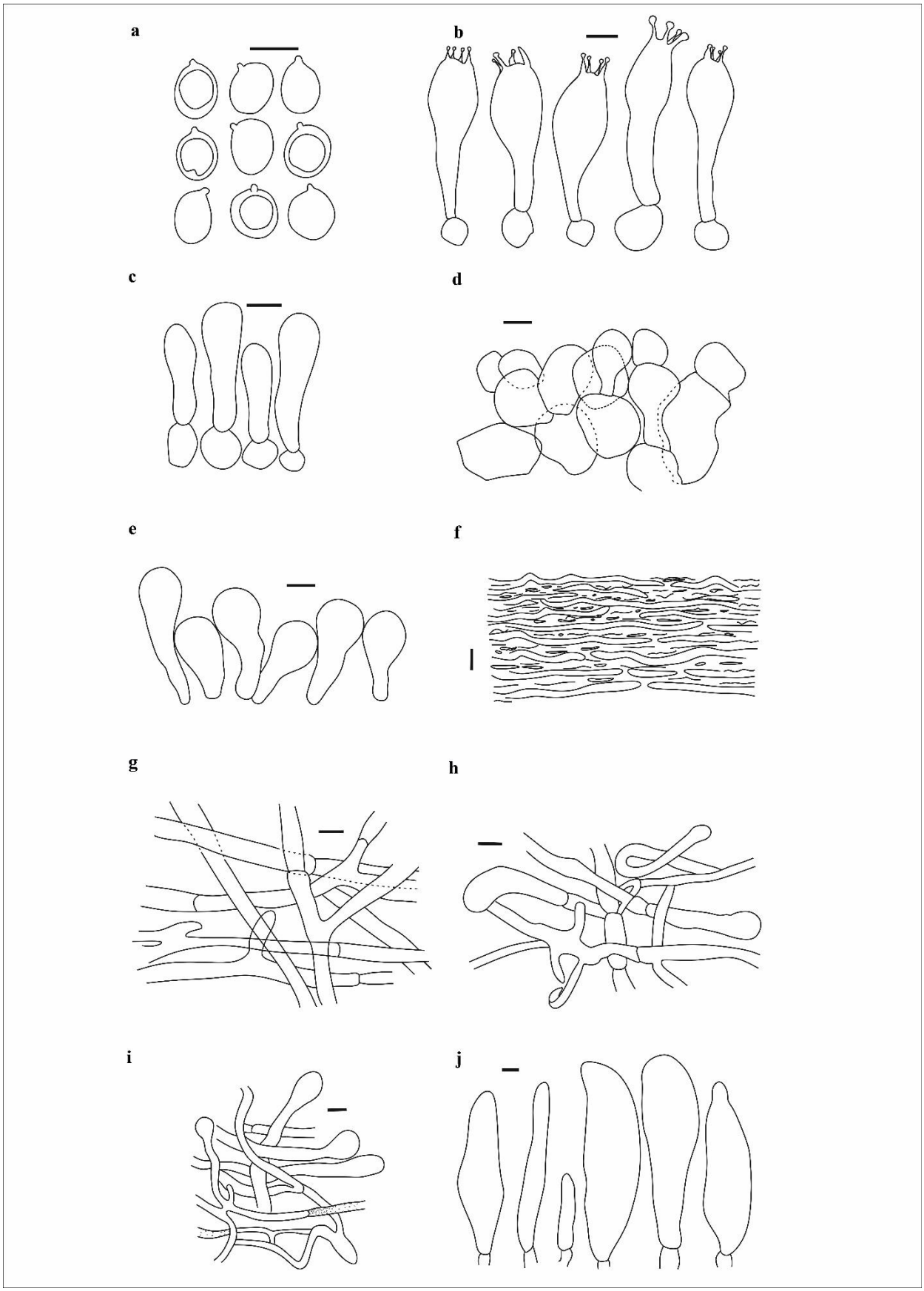

Fig. 5. *Amanita vidua*. **a**. Spores, **b**. basidia, **c**. basidioles, **d**. cells of subhymenyum, **e**. elements of lamellae edge, **f**. suprapellis, **g**. subpellis, **h**. elements of volva, **i**. elements of annulus, **j**. terminal cells of subpellis (scale bars: 10 μm).

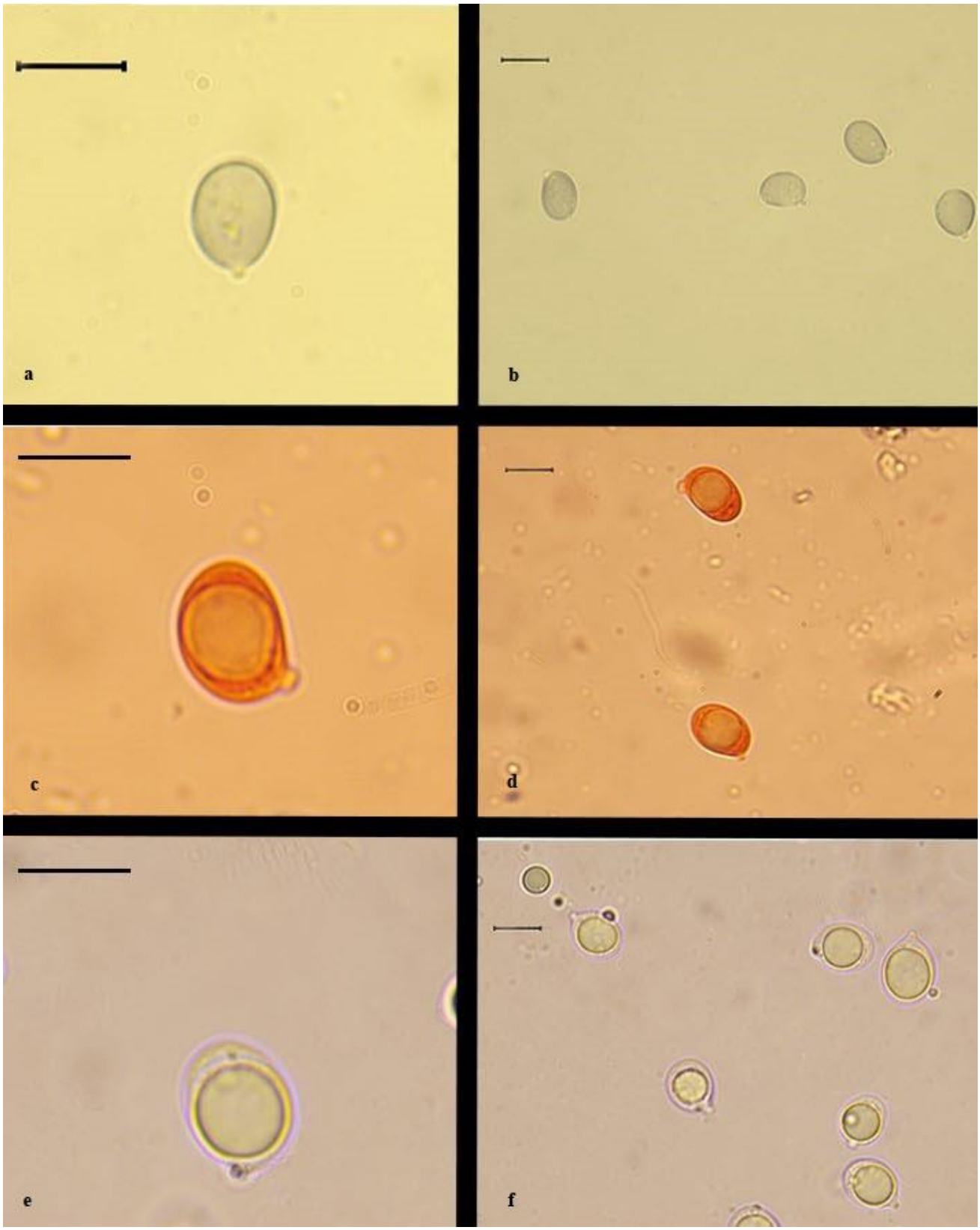

Fig. 6. Spores of *Amanita vidua*. **a, b.** In Melzer's reagent, **c, d.** in Congo red, **e, f.** in 5% KOH (scale bars: 10 µm).

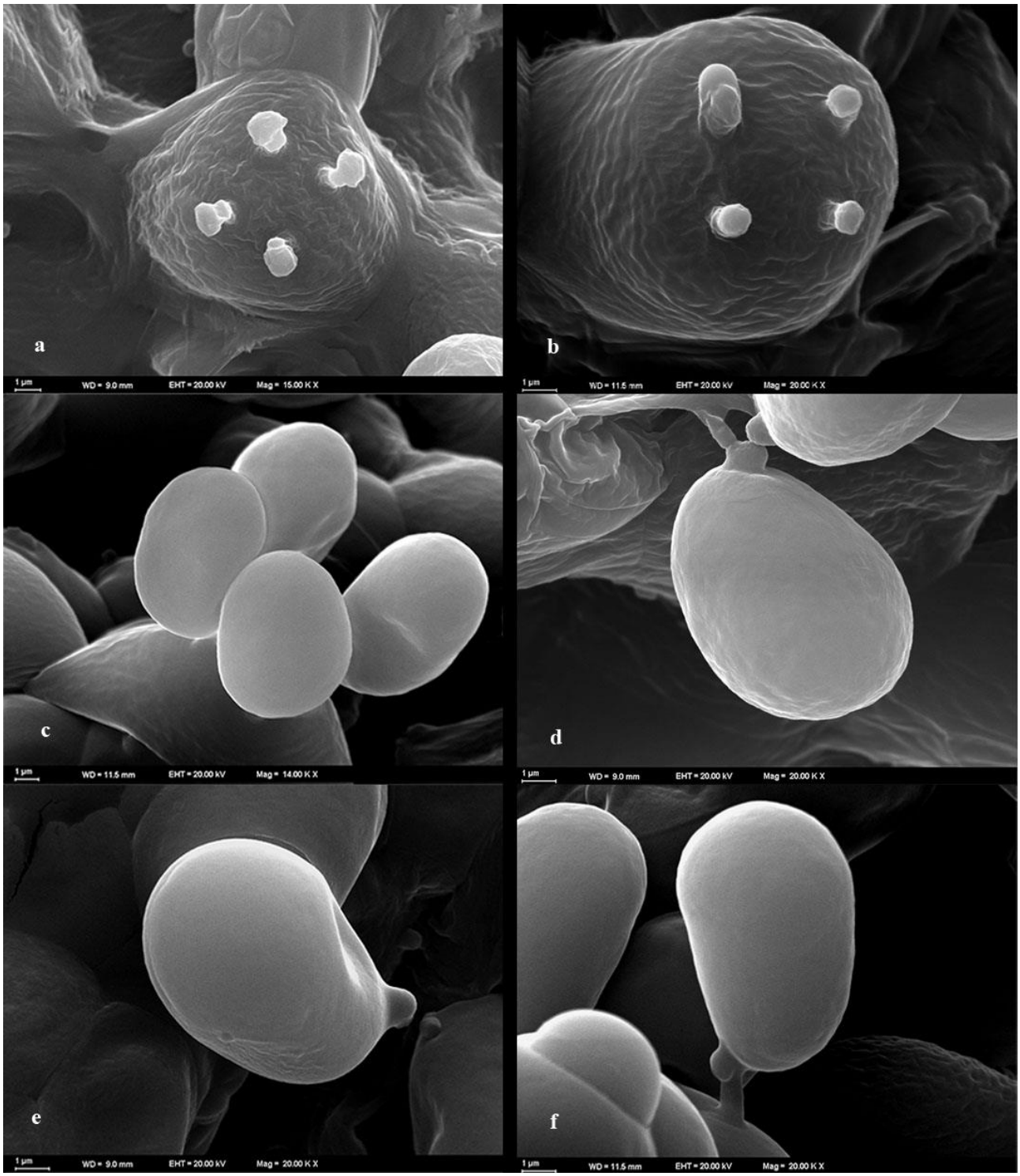

Fig. 7. SEM photographs of *A. vidua*. **a, b.** Top view of the basidium, **c.** four spores on basidium, **d-f.** spores.

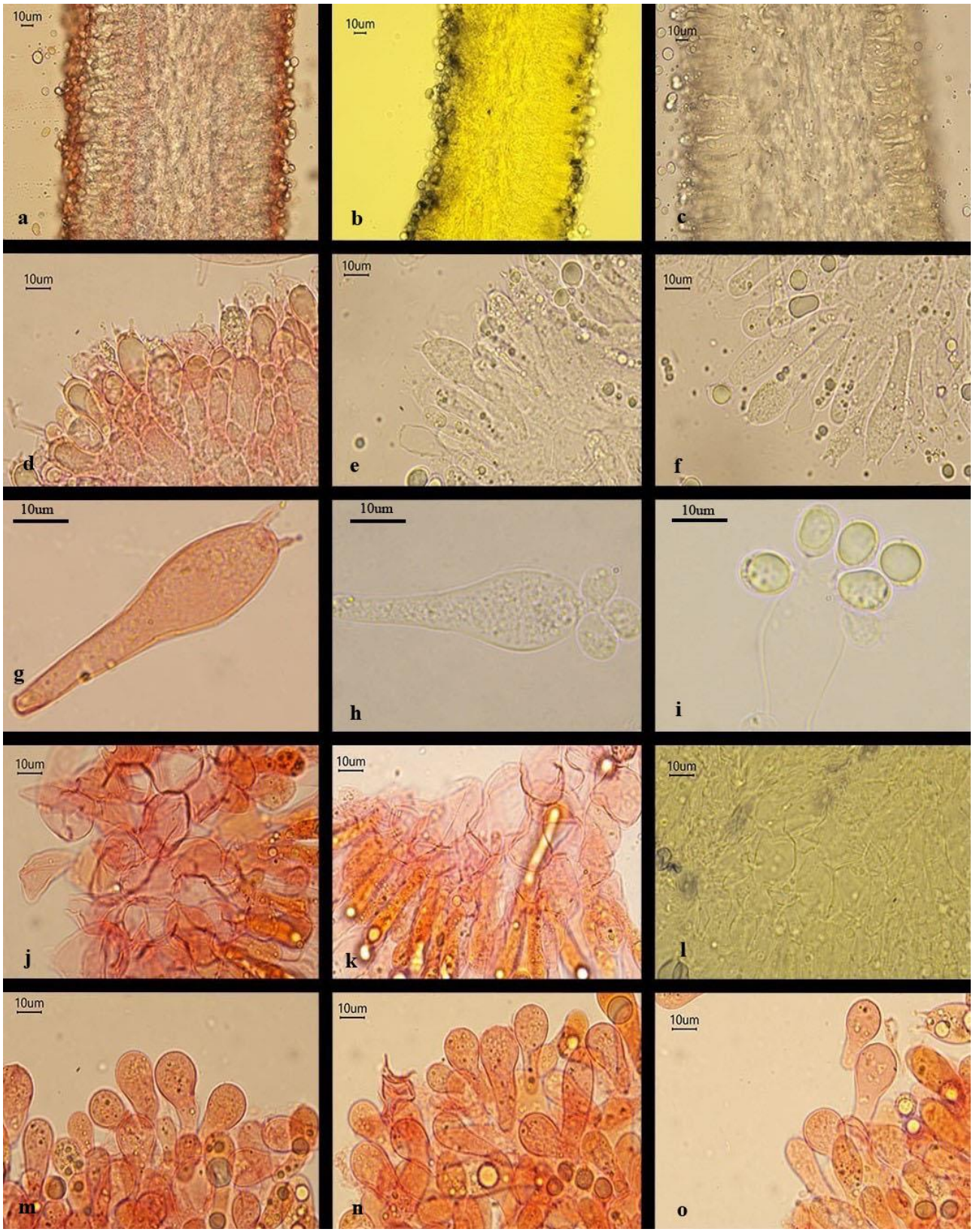

Fig. 8. Microscopic appearance of *A. vidua*. **a-c.** Hymenophoral trama, **d-f.** hymenium, **g-i.** a single basidium, **j-l.** subhymenium, **m-o.** lamellae edge.

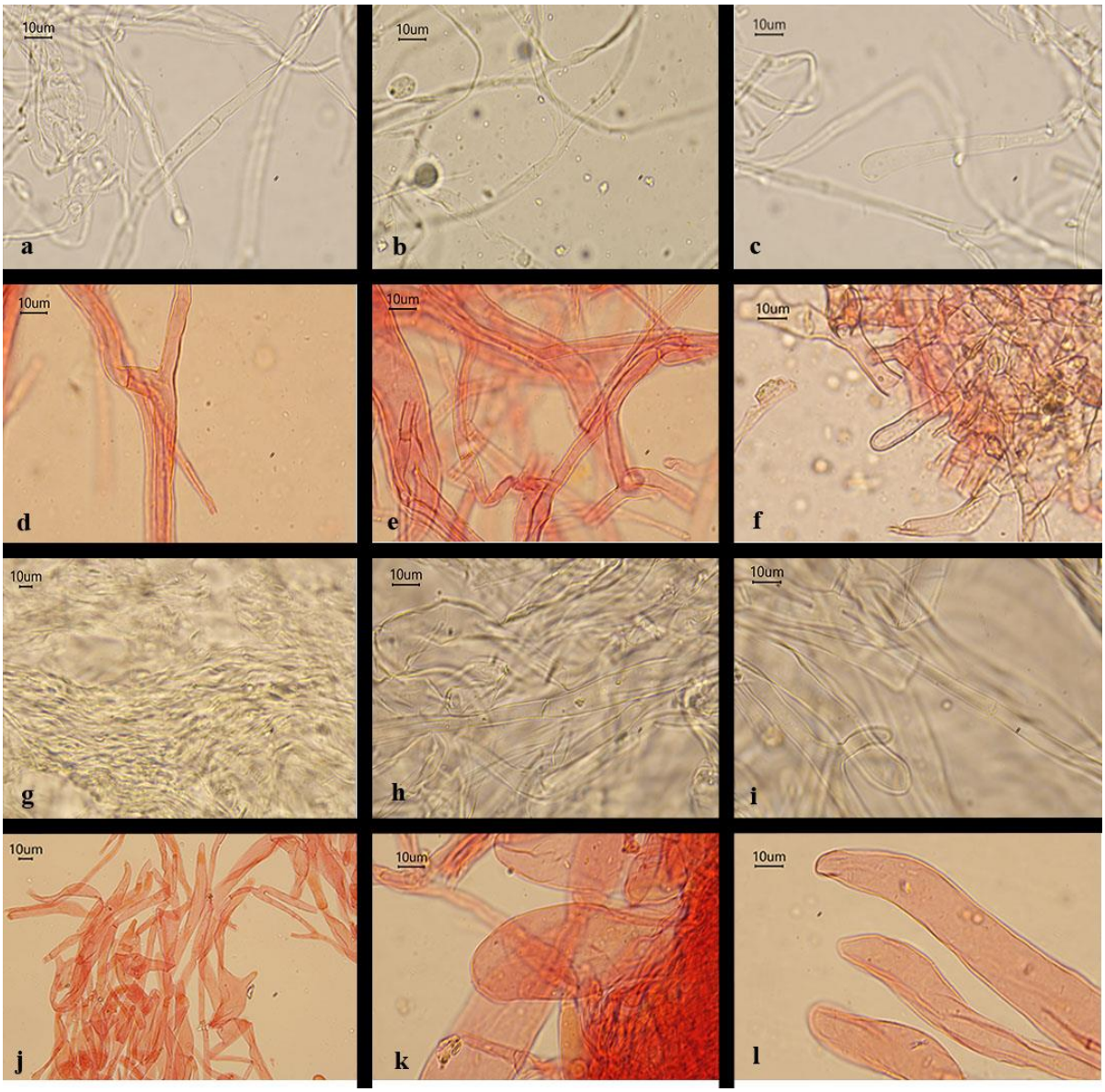

Fig. 9. Microscopic appearance of *A. vidua*. **a-c.** Partial veil (annulus), **d-f.** universal veil (volva), **g.** suprapellis, **h, i.** subpellis, **j-l.** terminal elements of subpellis.

Ecology and distribution: *Amanita vidua* typically appears in the spring months from April to early June. It is likely to form a symbiotic relationship with Mediterranean oak species such as *Quercus ilex subsp. ballota* (Desf.) Samp, *Q. pyrenaica* Willd, and *Q. suber* L., establishing ectotrophic mycorrhizae with them. Occasionally, it may also be associated with other trees like *Castanea*, *Fagus*, and *Pinus*. It is primarily observed on acidic soils within the Mediterranean region, including Lebanon in Asia, as well as some European countries (France, Italy, and Spain). The species has also been reported in Morocco (Alvarado *et al.* 2022).

Material examined: Türkiye-Uşak, Yeşildere village, on calcareous soils, under the Valonia oak (*Quercus ithaburensis* Decne subsp. *macrolepis* (Kotschy) Hedge & Yalt.), 38° 35' 21" N, 29°17' 56" E, 1005 m, 02.06.2023, ANK Akata & Kaya 007

Evolutionary History of ANK Akata & Kaya 007

The evolutionary history of the specimen ANK Akata & Kaya 007 was investigated based on its nrITS rDNA and *TEF1a* gene sequences. These sequences were obtained through standard molecular techniques and deposited in the NCBI GenBank with the accession numbers OR293358 and PP068301 for ITS rDNA region and *TEF1a* gene, respectively. To study the evolutionary relationships of ANK Akata & Kaya 007 within 32 fungal specimens, several nrITS rDNA and *TEF1a* gene sequences from other members of the *Amanita* genus were selected as representatives for ingroup comparison. The nrITS rDNA sequence of *Limacella subtropicana* A. Izhar, Niazi, M. Asif, Haqnawaz, H. Bashir & Khalid and a *TEF1a* gene sequence of *L. glioderma* (Fr.) Maire were chosen as the outgroup representatives. The molecular phylogenetic analysis utilizing both the ITS rDNA and *TEF1a* gene sequences identified four distinct clades,

along with the outgroups. Clade 1 and Clade 3 comprised different isolates of *Amanita vidua*, including the type material (LIP0401591), and the specimen ANK Akata & Kaya 007 in the phylogenetic trees constructed using the ITS rDNA and *TEF1a* gene sequences. The rest of the ingroup samples, used to build both phylogenetic trees, grouped into three different clades comprising other *Amanita* species, namely *A. phalloides*, *A. virosa*, and *A. verna*. *Limacella subtropicana* in the ITS rDNA tree and *L. glioderma* in *TEF1a* gene tree formed a separate branch outside the main clades, indicating their role as predicted outgroups. The phylogenetic trees constructed with ITS rDNA and TEF1a gene sequences had the highest log-likelihood values of -4701.80 and -2044.88 respectively. BLAST analyses using the nuclear ITS rDNA and *TEF1a* gene sequences of ANK Akata & Kaya 007 showed similarity rates exceeding 99% with different *A. vidua* isolates, including the type material (Alvarado *et al.* 2022). The phylogenetic analyses further supported the close relationship between this specimen and *A. vidua*, with a high branch bootstrap rate demonstrating the reliability of the grouping.

Discussion

Amanita vidua, which closely resembles *A. verna* , is often found fruiting in the same habitats as *A. verna*. It can be distinguished from *A. verna* by several key characteristics. One of the primary differences is the absence of a yellow reaction in all of its tissues when treated with KOH. Additionally, *A. vidua* has a stipe that is less noticeably bulbous compared to that of *A. verna*. In terms of the pileus, *A. vidua* often exhibits an early ochraceous tint and tends to be umbonate, which is a distinctive feature compared to the typically uncolored cap of *A. verna*. These subtle morphological differences are crucial to distinguish *A. vidua* from *A. verna*, especially in areas where their habitats overlap (Alvarado *et al.* 2022).

In the study conducted by Alvarado *et al.* (2022), comprehensive descriptions of morphological traits of *A. vidua* samples have been extensively documented, including the specific features of some macroscopic structures, alongside the properties and dimensions of spores, basidia, and the microscopic structures of the hymenium and pileipellis. Additionally, detailed accounts of both the universal veil and the partial veil have been meticulously examined. Table 1. provides a thorough comparison between the specimens of *A. vidua* analyzed in this study and those included in Alvarado *et al.* (2022). It meticulously outlines the dimensions of various structures observed in our samples, covering aspects such as the pileus, stipe, spores, and basidia, along with other microscopic elements found in the hymenium, pileus, annulus, and volva. This comparison is detailed, highlighting the similarities and differences in measurements and characteristics between the present and the type specimens.

The comparison of macroscopic and microscopic features of *A. vidua* specimens with those reported by Alvarado *et al.* (2022) reveals both congruencies and distinctions. Macroscopically, the dimensions align closely with previous findings, establishing a consistent framework for identifying these structures. However, our analysis presents notable discrepancies, particularly in the dimensions and morphology of certain microscopic elements.

Table 1. Comparison of some measurements of the morphological structures of *A. vidua*.

Dimensions	Alvarado *et al.* 2022	Current study
Pileus	not provided	60-80 mm broad
Stipe	75-160 × 10-18 mm	90-130 × 14-19 mm
Spores	(8.8-) 9.0-10.8 (-11.2) × (6.8-) 7.2-8.5 (-9.1) µm	(9.7-) 9.9-11.8 (-12.3) × (7.8-) 8-9 (-9.4) µm
Spores (Q-values)	Q = 1.15-1.30 (-1.60), Qav = 1.2	Q = 1.16-1.40 (-1.47), Qav = 1.32
Basidia	32-58 × 9-12 µm	42-64 × 12-18 µm
Subhymenium elements	15-25 × 12-20 µm	17-32 × 13-24 µm
Hymenophoral trama	(2.5-5 µm wide) intermixed with wider hyphae (7-11 µm)	3-5 µm, mixed with wider hyphae (8-12 µm)
Lamellae edges	30-38 × 11-14 µm	29-41 × 13-18 µm
Annulus (hyphae)	2-8 µm broad	4-8 µm
Annulus (sphaeropedunculate elements)	12-15 × 9-11 µm	22-45 × 8-16 µm.
Volva (hyphae)	3-7.5 µm broad	3-9 µm
Volva (inflated elements)	up to 45 µm broad	up to 20 µm broad
Suprapellis	2-5 µm broad	2-5 µm broad
Subpellis	1-2.5 µm broad, alongside some wider hyphae up to 5 (-7) µm	2-5 µm broad , some wider hyphae up to 10 µm broad
Terminal cells of subpellis	not provided	75-160 × 12-32

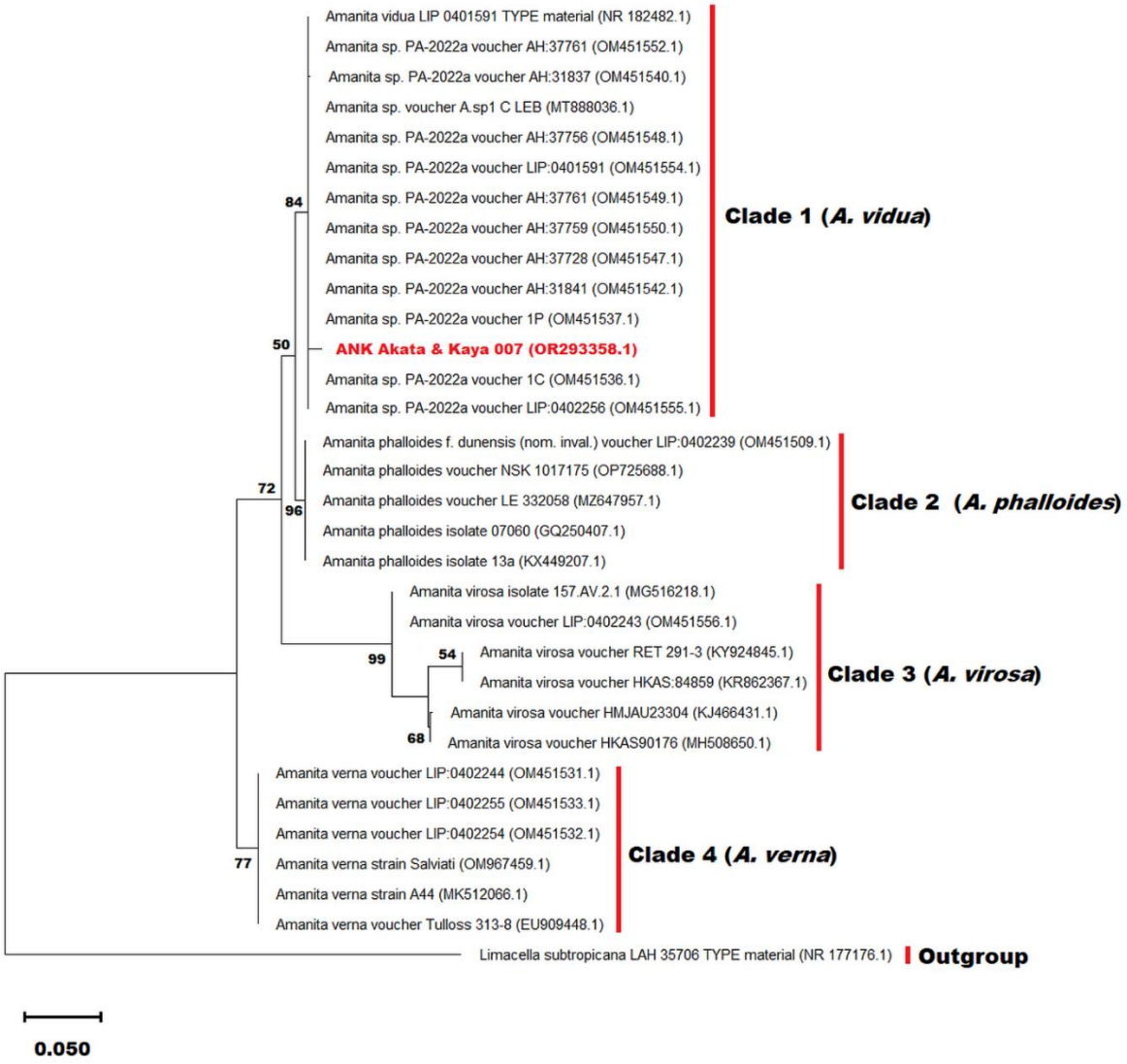

Fig. 10. A phylogenetic tree illustrating the evolutionary connections among 32 fungal specimens is presented using the nrITS rDNA region and the maximum likelihood (ML) method. Bootstrap rates are indicated for each branch to demonstrate the level of confidence. All sequences used in constructing the tree were sourced from the NCBI GenBank, except for ANK Akata & Kaya 007. Additionally, *Limacella subtropicana* was included in the phylogenetic tree as the outgroup representative. GenBank accession numbers are provided for each sequence, and the scale bar in the lower left signifies a genetic distance of 0.05.

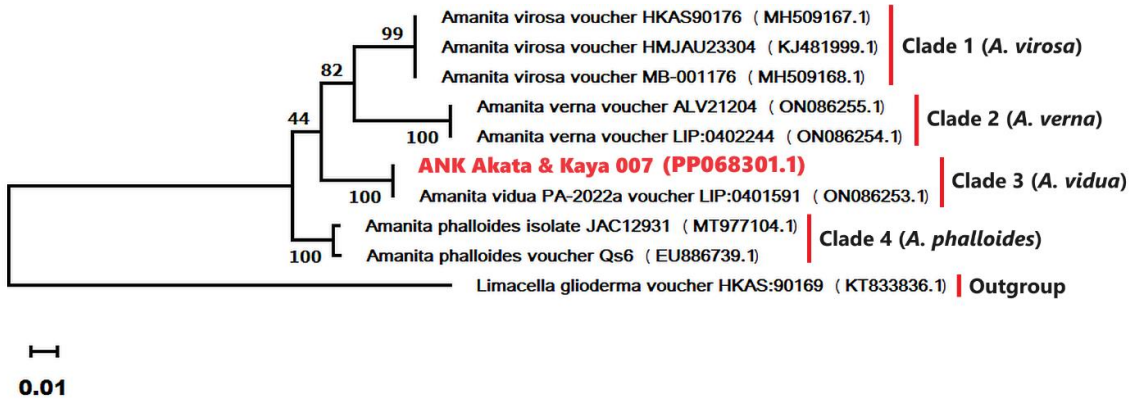

Fig. 11. A phylogenetic tree illustrating the evolutionary connections among 10 fungal specimens is presented using the partial sequence of the *TEF1a* gene and the maximum likelihood (ML) method. Bootstrap rates are indicated for each branch to demonstrate the level of confidence. All sequences used in constructing the tree were sourced from the NCBI GenBank, except for ANK Akata & Kaya 007. Additionally, *Limacella glioderma* was included in the phylogenetic tree as the outgroup representative. GenBank accession numbers are provided for each sequence, and the scale bar in the lower left signifies a genetic distance of 0.01.

Spore measurements in our specimens are larger, with dimensions of 9.9-11.8 × 8-9 µm and a mean aspect ratio (Qav) of 1.32, surpassing the previously reported range of 9.0-10.8 × 7.2-8.5 µm and a Qav of 1.2. Furthermore, basidium dimensions measured in our study (42-64 × 12-18 µm) exceed those documented by Alvarado *et al.* (32-58 × 9-12 µm), suggesting variations in the fungal reproductive structures that are critical for taxonomic distinctions. The subhymenium structures, described as lobate, rounded, or broadly elliptical, and sometimes angular or heart-shaped, were measured to be larger in our specimens (17-32 × 13-24 µm) compared to the previous study (15-25 × 12-20 µm). The consistency in the lamella edge structures is evident, as our findings (29-41 × 13-18 µm) closely resembled those (30-38 × 11-14 µm) reported by Alvarado *et al.* (2022), indicating a stable characteristic across various specimens. However, we observed differences in the terminal parts of the annulus and volva, with the former appearing larger and the latter narrower in our study compared to previous reports, highlighting variations in these structures. These discrepancies could potentially be attributed to environmental factors, genetic diversity, or developmental stages of the specimens, which may influence the morphological features of these fungal components. The pileipellis structure, reported by both studies as comprising two layers, showed compatibility regarding morphology and KOH reactions. However, our observations of the subpellis hyphae revealed wider dimensions, and notably, the suprapellis contained very long and wide terminal elements (75-160 × 12-32 µm) not mentioned previously, suggesting a degree of morphological plasticity or possibly overlooked variability within this species.

The recent study on Turkish samples of *A. vidua* highlights a subtle yet significant variation in the size of microscopic structures that, intriguingly, appear not to affect the process of species identification and classification. This variation may be indicative of a broader spectrum of intraspecific variability or perhaps an evolutionary adaptation within the species. Such a discrepancy raises important questions about the underlying mechanisms driving these differences and their implications for our understanding of species diversity and adaptability. It underscores the need for a more nuanced approach to the study of morphological characteristics, suggesting that even minor variations could have ecological or evolutionary significance. Consequently, these variances might unlock opportunities to investigate the genetic and environmental factors underlying the micromorphological diversity.

The morphological diversity of fungal species is significantly surpassed by their genetic diversity. Consequently, for more reliable identification of fungal species, genetic information is commonly employed in conjunction with traditional methods that rely solely on morphological data. To achieve this goal, various advantageous genetic markers, including rRNA gene regions such as nrITS, nrSSU, and nrLSU, as well as sequences of protein-coding genes such as translation elongation factor 1a (*TEF1a*) and tubulin (*TUB2*), have been used in molecular systematic studies for several decades (Raja *et al.* 2017). Among these markers, ITS is extensively employed for molecular taxonomic studies in the kingdom of fungi, providing valuable information. In our study, nuclear ITS rDNA and *TEF1a* gene sequences were used for the molecular identification of ANK Akata & Kaya 007, which revealed a similarity of more than 99% between reference sequences of *A. vidua* and the Turkish specimen (GenBank ID: OR293358.1 and PP068301.1) (Figs 10, 11).

Acknowledgement

Special thanks to Meltem Kurt (Türkiye) for her invaluable contribution to the project. Her dedication and expertise were instrumental in the detailed illustration of fresh specimens of acorns and a leaf of the Valonia oak, as well as the basidiomata of newly collected *Amanita vidua* specimens.

Ethics Committee Approval: Since the article does not contain any studies with human or animal subject, its approval to the ethics committee was not required.

Data Sharing Statement: Data available on reasonable request.

Author Contributions: Concept: I.A., E.K., E.Ş., İ.A., E.K., Design: I.A., E.K., Execution: I.A., E.K., E.Ş., Material supplying: I.A., E.K., Data acquisition: I.A., E.K., İ.A., E.K., Data analysis/interpretation: I.A., E.K., E.Ş., Writing: I.A., E.Ş., Critical review: I.A., E.Ş.

Conflict of Interest: The authors have no conflicts of interest to declare.

Funding: The study was supported by the Ankara University Research Funding Unit with project number FLO-2022-2709.

References

1. Akata, I., Kaya E., Yılmaz, İ., Bakırcı S. & Bayram, R. 2015. Türkiye'de Yetişen Alfa Amanitin İçeren Mantarlar. *Düzce Tıp Fakültesi Dergisi*, 17(1): 39-44.
2. Alvarado, P., Gasch-Illescas, A., Morel, S., Dagher-Kharrat, M.B. Moreno, G., Manjón, J.L., Carteret, X., Bellanger, J.M., Rapior, S., Gelardi, M. & Moreau P.A. 2022. *Amanita* Section *Phalloideae* Species in the Mediterranean Basin: Destroying Angels Reviewed. *Biology*, 11: 770. https://doi.org/10.3390/biology11050770
3. Chen, L., Cai, Y., Zhou, G., Shi, X., Su, J., Chen, G. & Lin, K. 2014. Rapid Sanger sequencing of the 16S rRNA gene for identification of some common pathogens. *PloS one*, 9(2): e88886. https://doi.org/10.1371/journal.pone.0088886
4. Codjia, J.E.I., Cai, Q., Zhou, S.W., Lou, H., Ryberg, M., Yorou, N.S. & Yang, Z.L. 2020. Morphology, multilocus phylogeny, and toxin analysis reveal *Amanita albolimbata*, the first lethal *Amanita* species from Benin, West Africa.

Frontiers in Microbiology, 11: 599047. https://doi.org/10.3389/fmicb.2020.599047

5. Codjia, J.E.I., Wang, P.M., Ryberg, M., Yorou, N.S. & Yang, Z.L. 2022. *Amanita* sect. *Phalloideae*: two interesting non-lethal species from West Africa. *Mycological Progress*, 21(3): 21-39. https://doi.org/10.1007/s11557-022-01778-0

6. Corrales, A., Henkel, T.W. & Smith, M.E. 2018. Ectomycorrhizal associations in the tropics – biogeography, diversity patterns, and ecosystem roles. *New Phytologist*, 220: 1076-1091. https://doi.org/10.1111/nph.15151

7. Cui, Y.Y., Cai, Q., Tang, L.P., Liu, J.W. & Yang, Z.L. 2018. The family *Amanitaceae*: molecular phylogeny, higher-rank taxonomy and the species in China. *Fungal Diversity*, 91: 5-230. https://doi.org/10.1007/s13225-018-0405-9

8. Felsenstein, J. 1985. Confidence limits on phylogenies: an approach using the bootstrap. *Evolution*, 39(4): 783-791.

9. Fraiture, A., Amalfi, M., Raspé, O., Kaya, E., Akata, I. & Degreef, J. 2019. Two new species of *Amanita* sect. Phalloideae from Africa, one of which is devoid of amatoxins and phallotoxins. *MycoKeys*, 53: 93-125. https://doi.org/10.3897/mycokeys.53.34560

10. Kumar, S., Stecher, G., Li, M., Knyaz, C. & Tamura, K. 2018. MEGA X: molecular evolutionary genetics analysis across computing platforms. *Molecular Biology and Evolution*, 35(6): 1547-1549. https://doi.org/10.1093/molbev/msy096

11. Kimura, M. 1980. A simple method for estimating evolutionary rate of base substitutions through comparative studies of nucleotide sequences. *Journal of Molecular Evolution*, 16: 111-120. https://doi.org/10.1007/BF01731581

12. Martin, K.J. & Rygiewicz, P.T. 2005. Fungal-specific PCR primers developed for analysis of the ITS region of environmental DNA extracts. *BMC Microbiology*, 5(28): 1-12. https://doi.org/10.1186/1471-2180-5-28

13. Raja, H.A., Miller, A.N., Pearce, C.J. & Oberlies, N.H. 2017. Fungal identification using molecular tools: a primer for the natural products research community. *Journal of Natural Products*, 80(3): 756-770. https://doi.org/10.1021/acs.jnatprod.6b01085

14. Rehner, S.A. & Buckley, E. 2005. A *Beauveria* phylogeny inferred from nuclear ITS and EF1-α sequences: evidence for cryptic diversification and links to *Cordyceps* teleomorphs. *Mycologia*, 97: 84-98. https://doi.org/10.3852/mycologia.97.1.84

15. Rogers, S.O. & Bendich, A.J. 1994. Extraction of total cellular DNA from plants, algae and fungi. pp. 183-190. In: Gelvin, S.B. & Schilperoort, R.A. (eds). *Plant Molecular Biology Manual*. Springer Netherlands, Dordrecht, 598 pp.

16. Sesli, E. 2022. *Amanita spadicea*: Türkiye Mikotası İçin Yeni Bir Kayıt. *Mantar Dergisi*, 13(2): 92-95. https://doi.org/10.30708.mantar.1094745

17. Sesli, E., Asan, A., Selçuk, F., Arabacı Günyar, Ö., Akata, I., Akgül, H., Aktaş, S., Alkan, S., Allı, H., Aydoğdu, H., Berikten, D., Demirel, K., Demirel, R., Doğan, H.H., Erdoğdu, M., Ergül, C.C., Eroğlu, G., Giray, G.., Halik Uztan, A., Kabaktepe, Ş., Kadaifçiler, D., Kalyoncu, F., Karaltı, İ., Kaşık, G., Kaya, A., Keleş, A., Kırbağ, S., Kıvanç, M., Ocak, İ., Ökten, S., Özkale, E., Öztürk, C., Sevindik, M., Şen, B., Şen, İ., Türkekul, İ., Ulukapı, M., Uzun, Ya., Uzun, Yu. & Yoltaş, A. 2020. *Türkiye Mantarları Listesi*. Ali Nihat Gökyiğit Vakfı Yayını, İstanbul, 1177 pp.

18. Tamura, K. 1992. Estimation of the number of nucleotide substitutions when there are strong transition-transversion and G + C-content biases. *Molecular Biology and Evolution*, 9: 678-687. https://doi.org/10.1093/oxfordjournals.molbev.a040752

19. Thongbai, B., Miller. S.L., Stadler, M., Wittstein, K., Hyde, K.D., Lumyong, S. & Raspe, O. 2017. Study of three interesting *Amanita* species from Thailand: Morphology, multiple-gene phylogeny, and toxin analysis. *PloS one*, 12(8): e0182131. https://doi.org/10.1371/journal.pone.0182131

20. White, T.J., Bruns, TD, Lee, S. & Taylor, J.W. 1990. Amplification and direct sequencing of fungal ribosomal RNA genes for phylogenetics. pp. 315-322. In: Innis, M.A. & Gelfand, D.H. (eds). *PCR Protocols: A Guide to Methods and Applications*. Academic Press, London, 482 pp.